Chaos, ergodicity, and the thermodynamics of lower-dimensional time-independent Hamiltonian systems

Henry E. Kandrup*
Department of Astronomy, Department of Physics, and Institute for Fundamental Theory, University of Florida, Gainesville, Florida 32611

Ioannis V. Sideris†
Department of Astronomy, University of Florida, Gainesville, Florida 32611

Courtlandt L. Bohn‡
Fermilab, Batavia, Illinois 60510

(Received 16 August 2001; published 20 December 2001)

This paper uses the assumptions of ergodicity and a microcanonical distribution to compute estimates of the largest Lyapunov exponents in lower-dimensional Hamiltonian systems. That the resulting estimates are in reasonable agreement with the actual values computed numerically corroborates the intuition that chaos in such systems can be understood as arising generically from a parametric instability and that this instability may be modeled by a stochastic-oscillator equation [cf. Casetti, Clementi, and Pettini, Phys. Rev. E **54**, 5969 (1996)], linearized perturbations of a chaotic orbit satisfying a harmonic-oscillator equation with a randomly varying frequency.

DOI: 10.1103/PhysRevE.65.016214 PACS number(s): 05.45.−a, 02.40.−k, 05.20.−y

I. INTRODUCTION AND MOTIVATION

By definition, Lyapunov exponents probe the average linear instability of chaotic orbits in an asymptotic $t\rightarrow\infty$ limit [1]. Their computation thus involves solving a matrix harmonic-oscillator equation with characteristic frequencies that vary in time. In the context of a geometric description—which is convenient but by no means necessary—this equation can be reinterpreted as a Jacobi equation (i.e., equation of geodesic deviation) for motion in an appropriately defined curved space, e.g., by introducing the Eisenhart metric [2].

It has been long known [3,4] that geodesic flows in a space with everywhere negative curvature are unstable in the sense that nearby orbits diverge exponentially; and, for this reason, there was an implicit assumption in much earlier work that chaos could often be understood as a manifestation of negative curvature. However, as emphasized by Pettini [5], in many systems chaos cannot be attributed to negative curvature. In many cases, the average curvature is positive; and indeed, there are many known examples of nonintegrable Hamiltonian systems (e.g., the finite-order truncations of the Toda [6] potential) which admit large measures of chaos even though the curvature is everywhere positive. The curvature associated with the Eisenhart metric can be negative only if the second derivative of the potential becomes negative. Instead, it would seem natural to understand chaos as reflecting a parametric instability.

The Jacobi equation for a regular periodic orbit reduces to a multidimensional Hill equation, i.e., a harmonic-oscillator equation with frequencies that exhibit a periodic time dependence. For certain amplitudes and periodicities, the solutions to such an equation remain bounded (or grow at most as a power law in time), this corresponding to stable periodic orbits. However, for other amplitudes and periodicities, the solutions grow exponentially, this corresponding instead to an unstable periodic orbit [7].

Since chaotic orbits are aperiodic and (in some sense) ''random,'' one might instead suppose that one can model the Jacobi equation describing a linearized perturbation of a chaotic orbit as a *stochastic* harmonic-oscillator equation, in which the time-dependent frequencies vary in a random fashion. Given this assumption, the key issue becomes one of identifying the stochastic process, i.e., the form of the colored noise, which can capture correctly solutions to the Jacobi equation.

If, for fixed potential and energy, almost all of the constant energy hypersurface is chaotic, as is true generically for $D>2$ (provided that the energy E is the only time-independent constant of the motion), it would seem reasonable to infer that the parameters for the oscillator equation should be estimatable assuming ergodicity. What this means is that one may assume an invariant measure corresponding to a uniform population of the constant energy hypersurface, i.e., a microcanonical distribution. If, furthermore, one is concerned with comparatively high-dimensional systems, the computationally awkward description in terms of a microcanonical distribution can be replaced by a more user-friendly description based on a canonical distribution: In the spirit of ordinary thermodynamics, one may argue that the canonical and microcanonical ensembles should yield nearly identical results in the large D limit.

Given this logic, Casetti, Clementi, and Pettini [8] developed a ''thermodynamic'' theory of chaos that they used to obtain very good estimates of the values of the largest Lyapunov exponents for two well-studied physical systems.

*Electronic address: kandrup@astro.ufl.edu
†Electronic address: sideris@astro.ufl.edu
‡Electronic address: clbohn@fnal.gov

To do this, they (i) extracted from the full D-dimensional Jacobi equation an ''isotropized'' one-dimensional oscillator equation that they argued should capture the chaotic behavior of typical orbits; (ii) derived the statistics of their assumed stochastic process in the context of a canonical ensemble description; and then (iii) showed that, for two seemingly generic models, solutions to the resulting equation yield reasonable estimates of the largest Lyapunov exponent, at least for $D>100$ or so.

An obvious question is whether this logic may also be exploited to provide reasonable estimates of the largest Lyapunov exponent for lower-dimensional systems, say $D=2$ or $D=3$. As discussed in the concluding section, there are a variety of settings where it would be convenient if one could estimate these values without resorting to detailed numerical computations. Arguably, however, this is *not* the most important point. Rather, the foremost objective is to implement a simple physical picture of the origins of chaos in lower-dimensional Hamiltonian systems. To the extent that the Casetti *et al.* proposal, or some variant thereof, can provide reasonable estimates of Lyapunov exponents in these systems, one would seem justified in visualizing chaos as arising from a parametric instability manifested by a stochastic-oscillator equation. In other words, one will have a clear alternative paradigm in terms of which to interpret the origins of chaos in lower-dimensional Hamiltonian systems.

II. AN ILLUSTRATIVE EXAMPLE

The validity of the formula for the largest Lyapunov exponent derived by Casetti *et al.* was tested for one simple toy model. The model is motivated by recent observations of elliptical galaxies, which suggest that these objects may exhibit significant deviations from axisymmetry and that they often have a high-density cusp at their centroids, perhaps associated with the presence of a supermassive black hole. The stars in a real galaxy populate a $6N$-dimensional phase space, with N denoting the number of stars in the system. Considering that fine structure due to localized irregularities and granularity will take a long time to manifest itself, it is of interest to model the system in terms of its coarse-grained six-dimensional phase space in expectation that the time scale associated with the coarse-grained potential will represent the shortest time scale for macroscopic evolution. Thus, a model potential for such systems comprises the sum of an anisotropic harmonic potential and a spherical Plummer potential,

$$V(x,y,z)=\tfrac{1}{2}(a^2x^2+b^2y^2+c^2z^2)-\frac{M_{\rm BH}}{\sqrt{r^2+\epsilon^2}}, \qquad (2.1)$$

with $r^2=x^2+y^2+z^2$, $a^2=1-\Delta$, $b^2=1$, and $c^2=1+\Delta$. Δ parametrizes the ellipsoidal geometry, and ϵ functions as a ''softening parameter'' that is set at $\epsilon=10^{-2}$ for numerical simulations.

The theory of Casetti *et al.*, described in Sec. IVA below is analytic, and within this formalism, ϵ acts as a ''free parameter'' that reflects uncertainty about the detailed dynamical properties of the phase space. One knows *a priori* that far from $M_{\rm BH}$ the potential is approximately quadratic in the coordinates, and close to $M_{\rm BH}$ it is approximately spherically symmetric; the orbits are accordingly quasiregular in these regions wherein there will be almost no chaotic mixing. The theory correctly predicts zero chaotic mixing in a harmonic-oscillator potential, thereby incorporating the former circumstance, but it also incorrectly predicts nonzero chaotic mixing in the spherically symmetric Plummer potential that dominates near $M_{\rm BH}$. Thus, a nonzero ϵ ''regularizes'' orbits near the black hole. In view of these considerations, the value of ϵ used in the theory was chosen by requiring the magnitude of the harmonic potential to be comparable to a tenth of that of the Plummer potential at distances ''$r=\epsilon$'' from the centroid. The specific choice is $\epsilon=0.5M_{\rm BH}^{1/3}$.

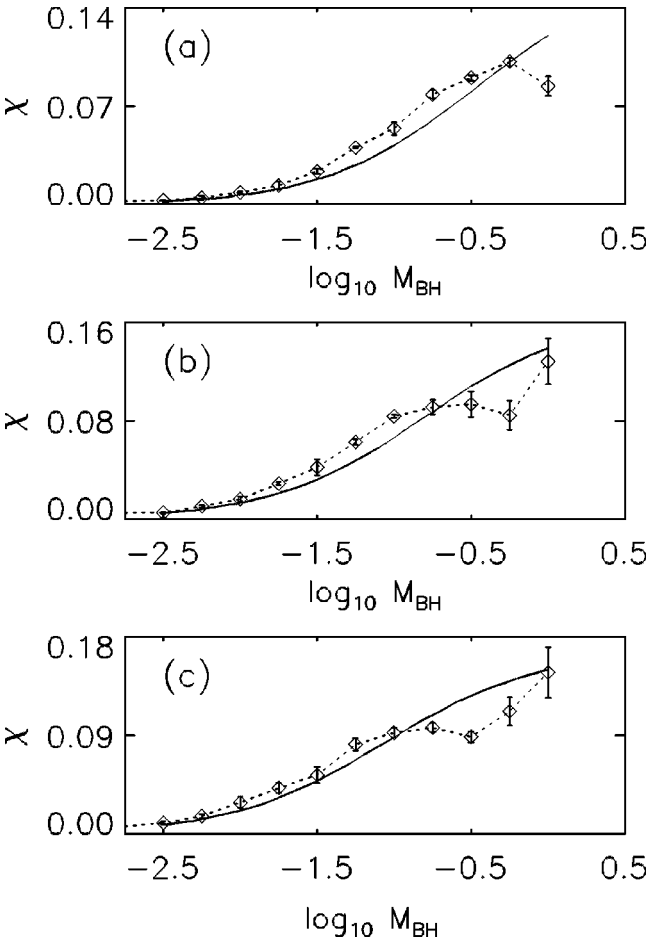

FIG. 1. (a) Numerical (diamonds) and analytic (solid line) estimates of the largest Lyapunov exponent for chaotic orbits evolved in the three-dimensional galactic potential (2.1) with $a^2=0.75$, $b^2=1.0$, and $c^2=1.25$ as a function of black-hole mass $M_{\rm BH}$ for total particle energy $E=1.0$. (b) The same for $E=0.6$. (c) $E=0.4$.

Figure 1 compares the ''true'' Lyapunov exponents computed via numerical simulations with estimates of the largest Lyapunov exponent derived using the Cassetti *et al.* formalism, Eqs. (4.12), (4.15), and (4.16) below. The numerical studies are described in detail in Ref. [9], and the numerically generated curves derive from Fig. 5 in that paper. The figure shows how the Lyapunov exponents pertaining to chaotic orbits scale against black-hole mass and total particle

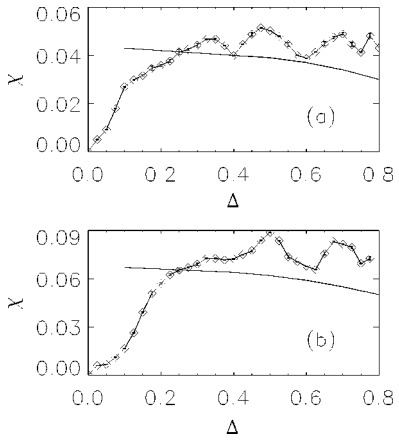

FIG. 2. (a) Numerical (diamonds) and analytic (solid line) estimates of the largest Lyapunov exponent for chaotic orbits evolved in the three-dimensional galactic potential (2.1) *i*th $M_{\rm BH}=0.1$ and $a^2=1-\Delta$, $b^2=1$, $c^2=1+\Delta$ as a function of Δ for total particle energy $E=1.0$. (b) The same for $E=0.6$.

energy E. Interestingly, the analytic results agree closely with the numerical results, particularly for intermediate-to-small values of $M_{\rm BH}$. The agreement is still reasonable for large values of $M_{\rm BH}$ (values that are in fact unphysically large), though the degree of agreement is less good. This is as expected in that a black-hole mass that is comparable to the ellipsoidal mass will establish sizeable regions of regularity over the constant-energy hypersurface, and the fraction of chaotic orbits will be correspondingly lower [9].

Figure 2 compares for fixed $M_{\rm BH}=0.1$ the numerical and analytic Lyapunov exponents versus ellipticity as parametrized by Δ. Again, the analytic technique is seen to yield reasonable estimates provided Δ is not too small. As Δ decreases to zero, the potential approaches spherical symmetry and is thereby integrable, supporting only regular orbits. Inasmuch as the fundamental assumption underlying the Casetti *et al.* formalism is that a substantial fraction of the orbits is globally chaotic, the formalism clearly breaks down for spherical symmetry. As discussed in Ref. [9], the fact that the numerical curves exhibit a great deal of structure not manifested by the analytic predictions reflects the fact that the phase space associated with the potential (2.1) is dominated by resonances with frequencies *a*, *b*, and *c* associated with the harmonic contribution that are completely independent of initial conditions.

The results of Figs. 1 and 2 suggest that the six-dimensional phase space governed by the toy potential (2.1) exhibits global chaos and associated rapid irreversible chaotic mixing over the bulk of the parameter space. Can the same be said for a lower-dimensional analog, i.e., one corresponding to the toy potential in which $z=p_z=0$? Figure 3, which provides the same information as Fig. 1, but now for a four-dimensional phase space, hints at the answer. One now sees the agreement between the numerical and analytic results to be less good, as would be expected, because the fraction of globally chaotic orbits is generally much reduced over the six-dimensional case. Nonetheless, the results are still comparable within a factor of two.

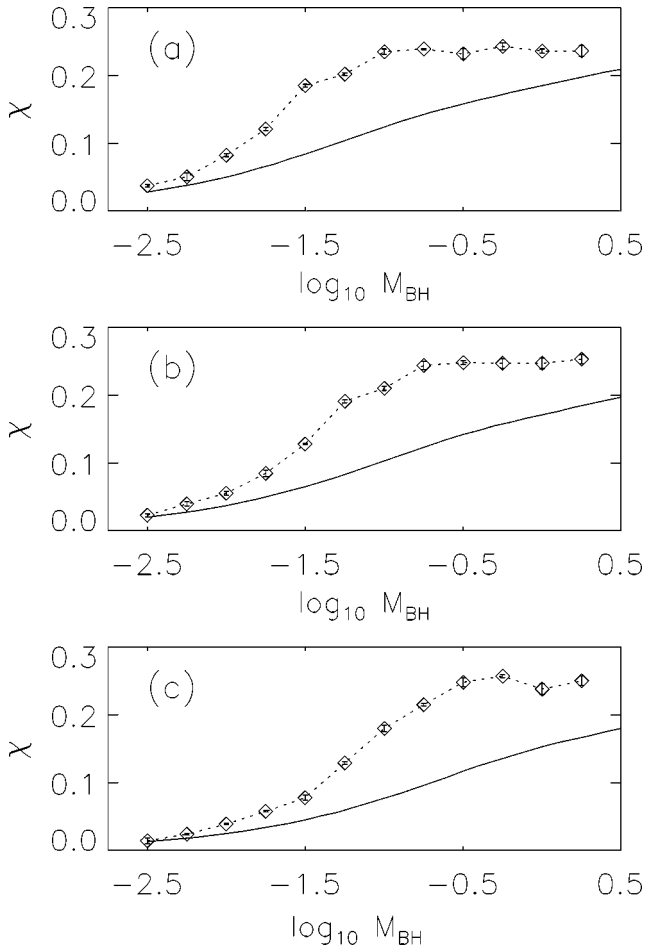

FIG. 3. Same as Fig. 1, but with all orbits restricted to the two-dimensional (x, y) plane.

III. THE SCOPE OF THIS PAPER

The obvious question is whether the striking agreement between theory and numerics described in the preceding section is simply a fortuitous accident, or whether it is in fact generic. Can the Casetti *et al.* analysis provide reasonable estimates of the largest Lyapunov exponent for generic lower-dimensional Hamiltonian systems?

Related to this is another important question: To what extent are the assumptions implemented by Casetti *et al.* justified for lower-dimensional systems? To the extent that they are *not* justified, one might expect either (i) that the final formula for χ that they derived is comparatively insensitive to (some of) the assumptions and/or (ii) that modifying these assumptions might lead to improved estimates.

These questions were addressed by a detailed exploration of orbits in the potentials discussed in Sec. II, as well as three other (classes of) potentials,

(1) The sixth-order truncation of the Toda lattice [6], a familiar two-dimensional potential,

$$V(x,y)=\tfrac{1}{2}(x^2+y^2)+x^2y-\tfrac{1}{3}y^3+\tfrac{1}{2}x^4+x^2y^2+\tfrac{1}{2}y^4+x^4y+\tfrac{2}{3}x^2y^3-\tfrac{1}{3}y^5+\tfrac{1}{5}x^6+x^4y^2+\tfrac{1}{3}x^2y^4+\tfrac{11}{45}y^6. \quad (3.1)$$

(2) A multidimensional generalization of the dihedral potential [10], for one particular set of parameter values, allowing for $D=2$ through $D=6$,

$$V(q_1,\ldots,q_D)=-\sum_{i=1}^{D} q_i^2+\frac{1}{4}\left(\sum_{i=1}^{D} q_i^2\right)^2-\frac{1}{4}\sum_{i<j=1}^{D} q_i^2 q_j^2. \tag{3.2}$$

(3) A generalization of the Fermi-Pasta-Ulam (FPU) β model [11] with

$$V(q_1,\ldots,q_D)=\sum_{i=1}^{D}\left[\tfrac{a}{2}[q_{i+1}-q_i]^2+\tfrac{b}{4}(q_{i+1}-q_i)^4\right], \tag{3.3}$$

with $q_{D+1}\equiv q_1$, allowing for $D=3$ through $D=6$ (the special case $D=2$ is integrable). For $a=1$, Eq. (3.3) reduces to the standard FPU model; for $a<0$, the potential admits extrema that are local maxima, so that the local mean curvature can become negative. The case $a=1$ and $b=0.1$ was considered by Casetti *et al.* for much larger values of D.

Section IV of this paper begins by providing a terse mathematical summary of the formalism introduced by Casetti *et al.* to estimate the values of the largest Lyapunov exponent in higher-dimensional systems. This mathematical structure is then restated in much simpler physical language and the resulting reformulation is used to suggest how their analysis could be reformulated for lower-dimensional systems. Section V summarizes the results of extensive simulations in the potentials (2.1) and (3.1)–(3.3), which were used to test the validity of the original assumptions. Section VI then turns to the actual values of Lyapunov exponents estimated using this general approach, considering both the ''true'' Lyapunov exponents, defined in a $t\to\infty$ limit, and short-time Lyapunov exponents [12] appropriate for orbit segments of comparatively short duration. Estimates of the latter for a variety of different orbit segments evolved in the same potential with the same energy reveals an important point: Even when the estimated short-time exponents $\chi_{\rm est}$ differ from the ''true'' exponents $\chi_{\rm num}$ computed numerically by as much as a factor of two, their values tend to be strongly correlated. For example, orbit segments for which $\chi_{\rm est}$ is especially small correspond, in general, to orbits for which the numerical $\chi_{\rm num}$ is also especially small. In this sense, it is clear that, even if the Casetti *et al.* formula for χ is not completely satisfactory, it *does* capture some important aspects of the flow. Section VII concludes by summarizing the principal conclusions and discussing potential implications and extensions.

IV. CHAOTIC MOTION AS A STOCHASTIC PARAMETRIC INSTABILITY

A. The proposal of Casetti, Clementi, and Pettini

The starting point is the reformulation of a time-independent Hamiltonian system as a geodesic flow in an appropriately defined curved space. This can be done in a variety of different ways, the best known of which involves implementing Maupertuis' Principle [13], which leads to the Jacobi metric. However, from a practical perspective, the most convenient choice is to work with the Eisenhart metric [2].

Given a D degree-of-freedom Hamiltonian system characterized by a Lagrangian

$$L=T-V=\tfrac{1}{2}a_{ij}\dot{q}^i\dot{q}^j-V(q^1,\ldots,q^D), \tag{4.1}$$

with motion defined on some manifold M, consider the extended manifold $M\times R^2$, with coordinates $(q^0,q^1,\ldots,q^D,q^{D+1})$, and introduce the Eisenhart metric

$$\begin{aligned} ds^2&=g_{\mu\nu}\,dx^\mu dx^\nu \\ &=a_{ij}\,dq^i\,dq^i-2V(q)dq^0\,dq^0+2\,dq^0\,dq^{D+1}. \end{aligned} \tag{4.2}$$

Setting $q^0=t$ and $q^{D+1}=t/2-\int_0^t dt' L(\mathbf{q},\dot{\mathbf{q}})$ yields $ds^2=dt^2$. Without loss of generality, one can set $a_{ij}=\delta_{ij}$, making the kinetic energy a sum of quadratic contributions $(\dot{q}^i)^2/2$, in which case the geodesic equations reduce to Newton's equations of motion. Correspondingly, the Riemann tensor simplifies greatly; its only nonvanishing components are

$$R_{0i0j}=\frac{\partial^2 V}{\partial q^i\partial q^j}, \tag{4.3}$$

and the Jacobi equation for a linearized perturbation becomes

$$\ddot{\xi}^i+\delta^{ij}R_{0j0k}\xi^k=0,\quad (i=1,\ldots,D). \tag{4.4}$$

Were the Riemann components entering into Eq. (4.4) everywhere negative, an arbitrary perturbation would always grow exponentially fast. Everywhere negative curvature implies chaotic behavior and positive Lyapunov exponents [3,4]. The important point, however, is that, because of parametric instability, one can have chaotic orbits with positive Lyapunov exponents even if the curvature is everywhere positive. If, following Casetti *et al.*, one assumes that the curvature varies ''randomly'' along a chaotic orbit, Eq. (4.5) reduces to a stochastic-oscillator equation of the form

$$\frac{d^2\xi^i}{dt^2}+k^i_j(t)\xi^j=0,\quad (i=1,\ldots,D), \tag{4.5}$$

where the matrix k^i_j is characterized completely by its statistical properties. However, it is well known that, even if k^i_j is positive definite for all times, ξ^i can grow exponentially [14].

Especially in high dimensions, matrix equations become difficult to solve either numerically or analytically. For this reason, Casetti *et al.* proceeded by replacing this D-dimensional equation with a simpler one-dimensional equation that aims to capture its ''average'' behavior. Formally, they start by observing that the Riemann tensor may be decomposed into two pieces

$$R^i_{jkl}=\frac{1}{D-1}(R_{ji}\delta^i_k-R_{jk}\delta^i_l)+W^i_{jkl}, \tag{4.6}$$

where R_{ij} is the Ricci tensor and W^i_{jk} is the Weyl projective tensor. For the case of an isotropic space, the Weyl tensor vanishes identically and $R_{jl}\dot{q}^j\dot{q}^l/(D-1)$ reduces to the (constant) sectional curvature. The crucial assumption then is that, even though the space is not isotropic, it should appear nearly isotropic when viewed on comparatively large scales. In the context of such a ''quasi-isotropic'' approximation, R^i_k and $w^i_k=\delta^{ij}W^l_{jlk}$ become diagonal, and Eq. (4.6) reduces to a one-dimensional equation of the form

$$\frac{d^2\xi}{dt^2}+k(t)\xi=0. \tag{4.7}$$

All that remains is to specify the statistical properties of the random process $k(t)$.

For a generic Hamiltonian system, the form of k could be quite complex. However, given the assumption that D is large, one might expect that the complicated details will largely wash out. Thus, Casetti *et al.* argue in the spirit of the central limits theorem that the curvature fluctuations in different directions may be approximated as nearly independent and, at any instant, Gaussianly distributed. It then follows that

$$\frac{d^2\xi}{dt^2}+\Omega\xi+\sigma\eta\xi=0, \tag{4.8}$$

where, in terms of the quantity $K=\partial^2V/\partial q^i\partial q_i\equiv\Delta V$, which has mean $\langle K\rangle$ and dispersion δK, the quantity $\Omega=\langle K\rangle/(D-1)$, $\sigma=\delta K/\sqrt{D-1}$, and η is Gaussian noise with zero mean and unit variance. The factors involving D reflect the fact that the curvature-driven motion in the ith direction is, on the average, ''shared'' by the $D-1$ orthogonal directions.

Presuming further that the flow is ergodic and that (almost) all orbits are chaotic, the quantities $\langle K\rangle$ and δK may be calculated assuming a uniform sampling of the constant energy hypersurface, i.e., a microcanonical distribution $\mu\propto\delta_D(H-E)$. Alternatively, for sufficiently high dimensions, one may proceed instead by assuming a canonical distribution which, for large D, is much simpler computationally although it should yield nearly identical results.

To complete the characterization of the random process $k(t)$, it remains to specify the autocorrelation function $\Gamma(t)$ or, at least, the autocorrelation time τ, which governs how rapidly the curvature fluctuates along the orbit. This, Casetti *et al.* provide using another geometric argument. On the one hand, they identify a time scale

$$\tau_1\approx\frac{\pi}{2\sqrt{\Omega+\sigma}} \tag{4.9}$$

corresponding to the typical time between successive conjugate points, i.e., points where the Jacobi field of geodesic deviation vanishes. On the other, they identify a time scale

$$\tau_2\approx\frac{\Omega^{1/2}}{\sigma} \tag{4.10}$$

corresponding to the length scale on which the fluctuations become comparable to the average curvature. They then select as an appropriate autocorrelation time a value τ satisfying

$$\tau^{-1}=2(\tau_1^{-1}+\tau_2^{-1}) \tag{4.11}$$

so that

$$2\tau=\frac{\pi\sqrt{\Omega}}{2\sqrt{\Omega(\Omega+\sigma)}+\pi\sigma}. \tag{4.12}$$

Casetti *et al.* suggest further that $\Gamma(t)$ might be well approximated by the oscillating function

$$\Gamma(t)=\frac{\Omega^2}{\pi}\frac{\sin\omega t}{\omega t}, \tag{4.13}$$

which yields an autocorrelation time

$$\tau=\frac{1}{2\omega}=\frac{\tau_{\rm osc}}{4\pi}, \tag{4.14}$$

with $\tau_{\rm osc}$ the oscillation period. However, this is largely irrelevant for their analysis. Granted the assumption of additive Gaussian noise, the form of the color only enters into the final expression for χ through the autocorrelation time τ[14].

Given a knowledge of τ and the first two moments, Eq. (4.8) may be solved analytically using a technique developed by van Kampen [14] to yield an estimated largest Lyapunov exponent

$$\chi=\frac{1}{2}\left(\Lambda-\frac{4\Omega}{3\Lambda}\right), \tag{4.15}$$

where

$$\Lambda=\left[2\sigma^2\tau+\sqrt{\left(\frac{4\Omega}{3}\right)^3+(2\sigma^2\tau)^2}\right]^{1/3}. \tag{4.16}$$

B. Applying this proposal to lower-dimensional Hamiltonian systems

The preceding may be reformulated without recourse to differential geometry in a setting that makes the physical content of the assumptions more transparent and, as such, makes it clearer which assumptions might prove suspect, especially for lower-dimensional systems.

The basic perturbation Eq. (4.5) may be derived trivially from the original Hamilton equations

$$\frac{dq^i}{dt}=\frac{\partial H}{\partial p_i}=\delta^{ij}p_j \tag{4.17}$$

and

$$\frac{dp_i}{dt}=-\frac{\partial H}{\partial q^i}=-\frac{\partial V}{\partial q^i} \tag{4.18}$$

associated with the Hamiltonian

$$H = T + V = \tfrac{1}{2}\delta^{ij} p_i p_j + V(q). \tag{4.19}$$

It is clear that the introduction of a small perturbation $q^i \rightarrow q^i + \xi^i$ and $p_i \rightarrow p_i + \zeta_i$ leads to evolution equations of the form

$$\frac{d\xi^i}{dt} = \delta^{ij}\zeta_j \quad \text{and} \quad \frac{d\zeta_i}{dt} = -\frac{\partial^2 V}{\partial q^i \partial q^j}\xi^j, \tag{4.20}$$

but combining these last two equations leads immediately to Eq. (4.4).

The crucial assumption underlying the entire Casetti *et al.* analysis is the assumption that, for the case of chaotic orbits, Eq. (4.4) can be modeled by a stochastic-oscillator equation. For the case of ''wildly chaotic'' orbits or orbit segments, which are far from periodic, this assumption would seem quite reasonable. However, in lower-dimensional systems one encounters the possibility of ''sticky'' [15] orbit segments that, albeit characterized by positive short-time Lyapunov exponents, are ''nearly regular'' in visual appearance and have Fourier spectra with most of the power concentrated at or near a few special frequencies [16]. This is especially common for $D=2$, where cantori [1] can serve as entropy barriers, confining a chaotic orbit near a regular island for surprisingly long times. To the extent that such orbit segments behave in a nearly regular fashion, the assumption of nearly random behavior is clearly suspect, and one might anticipate that a stochastic-oscillator equation cannot prove completely satisfactory. Alternatively, to the extent that this ''sticky'' behavior is rare, such an equation might be expected to provide a reasonable starting point.

The assumption of ''quasi-isotropy'' may also be understood in very simple physical terms: Instead of considering the D-dimensional Eq. (4.4), which involves the full second derivative matrix of V, it is assumed that, on the average, each direction in configuration space is statistically identical, so that one can consider instead D identical one-dimensional equations. In this context, the only question concerns the proper identification of the quantity to play the role of the squared frequency $k(t)$. The Casetti *et al.* prescription states that the relevant information about stability is contained in the trace of the second derivative matrix, so that $k(t)$ should be proportional to $\Delta V = \partial^2 V/\partial q^i \partial q_i$. The factor of $D-1$ entering into Eq. (4.8) reflects the fact that the perturbation driving the chaos is ''shared'' among $D-1$ dimensions. [Recall that, in a time-independent Hamiltonian system, there is always one direction of neutral stability corresponding to translation along the orbit from $q^i(t)$ to $q^i(t+\delta t)$.].

This assumption of quasi-isotropy seems especially reasonable for large D where, on average, different directions of the configuration space should look much the same, but becomes more suspect in lower dimensions. In principle, one can relax this assumption by working with the full matrix equation. As a practical matter, however, this becomes quite cumbersome for $D \gg 2$. For this reason, most of the following analysis will retain the assumption of quasi-isotropy. What happens when this assumption is relaxed for two-dimensional systems is considered briefly in Sec. VI. It would in fact appear that, at least for $D=2$, relaxing this assumption does not, in general, yield significant improvement in the estimated value of the largest Lyapunov exponent.

For generic Hamiltonian systems with large D, one anticipates that (almost) all the orbits on a constant-energy hypersurface are chaotic. Granted the assumption of ergodicity, it then follows that, over sufficiently long time scales, an orbit eventually samples a microcanonical distribution. This implies that, when estimating a Lyapunov exponent $\chi(E)$, as defined in an asymptotic $t \rightarrow \infty$ limit, one may assume that the statistical properties of the curvature experienced by an orbit are given correctly by a microcanonical distribution. By contrast, for lower-dimensional systems, especially $D=2$, one anticipates instead that a generic potential will admit a coexistence of large measures of both regular and chaotic orbits, so that the assumption of a microcanonical distribution is not justified. Rather, granted the assumption of ergodicity, one would anticipate the existence of a different invariant distribution, corresponding to a uniform population of those portions of the constant energy hypersurface that are accessible to a chaotic orbit with specified initial condition. It is not clear how this distribution could be computed analytically. However, as described in Sec. V, numerical approximations to this invariant distribution may be generated straightforwardly through a time-series analysis of orbits evolved numerically.

Even if a microcanical distribution is justified, the assumption of Gaussian fluctuations is problematic. For large D, this assumption may be motivated with a fair degree of rigor via a central limits theorem argument, supposing that the distribution of values of ΔV involves a convolution of D nearly independent distributions for the separate components $\partial^2 V/\partial q^i \partial q^i$ (no sum over indices). For very small D, this is clearly not justified, and the minimum value of D for which the Gaussian approximation *is* justified must depend to a certain extent on the form of the individual distributions. It will be seen in Sec. V that, for the model systems (3.2) and (3.3), the convergence towards a Gaussian is quite efficient, and that the distribution $N[\Delta V]$ is reasonably well fit by a Gaussian even for D as small as 3 or 4. It will also be seen that, at least for distributions $N[\Delta V]$ that are not too skew, deviations from a Gaussian do not change the estimated value of the largest Lyapunov exponent all that much.

The formula for the autocorrelation time τ motivated by Casetti *et al.* is somewhat *ad hoc* in that, unlike the other crucial inputs Ω and σ, it cannot be derived directly from a microcanonical distribution. However, the basic scaling implicit in τ may again be inferred relatively simply. As will be seen below, Ω and σ are typically comparable in magnitude. They both reflect statistical properties of ΔV and, as such, scale (within factors of order unity) as $\overline{V}/R^2$, where $\overline{V}$ represents a typical value of potential and R is a characteristic length scale, i.e., the size of the configuration space region probed by an orbit. Assuming ''virialization,'' i.e., that the mean potential and kinetic energies of the orbits are comparable in magnitude, it follows that $\overline{V} \sim v^2$, where v denotes a typical orbital speed. However, this implies that $\Omega \sim \sigma \sim v/R \equiv t_D^{-1}$, where t_D denotes a characteristic dynamical or

crossing time. Allowing for the fact that the characteristic scale on which V changes significantly is typically somewhat smaller than the size of region accessible to the orbit leads to the obvious physical conclusion that τ should be comparable to, but somewhat smaller than, the time required for an orbit to travel from one side of the system to another.

Implicit in the Casetti *et al.* analysis is the assumption that the stochastic process $k(t)$ corresponds to state-independent, additive noise, so that, e.g., the autocorrelation time τ on which the curvature changes is independent of the value of the curvature. Strictly speaking, this assumption cannot be correct. If, e.g., an orbit is in a region where V is especially small, its kinetic energy, and hence, its velocity, will be especially large, so that the orbit will move very quickly to a different region where V, and hence in general ΔV, is very different. If, instead, the orbit is in a region where V is especially large, it will move more slowly so that ΔV might be expected to change more slowly. The autocorrelation time τ of Eq. (4.13) represents an average over a variety of orbits with very different values of V. One might anticipate that these differences will tend to wash out for large D, but there is no obvious reason why this should be true for smaller D.

One final point. It is clear that, for small D, one cannot pass from a microcanonical to a canonical description. One must work directly with the microcanonical measure $\mu \propto \delta_D(H-E)$. This, however, is not a major problem. For a D degree of freedom system, the microcanonical distribution corresponds to a configuration space density

$$f(q^i) \propto \begin{cases} (E-V)^{(D-2)/2} & \text{if } V \leqslant E; \\ 0 & \text{if } V > E, \end{cases} \tag{4.21}$$

but, given this formula for f, it is straightforward, at least numerically, to compute the distribution $N[\Delta V]$ and/or any moments of the distribution.

V. TESTING THE BASIC ASSUMPTIONS

A. What was computed

To test the validity of the basic assumptions requires a comparison of real orbital data with predictions made assuming a microcanonical distribution. The requisite orbital data were generated and analyzed as follows.

For given choices of potential and total energy, a collection of $N=1000$ initial conditions were selected, and each of these was integrated into the future for a total time T corresponding to between $\sim$100 and 2000 characteristic crossing times t_D. The numerical integration simultaneously tracked the evolution of a small initial perturbation, periodically renormalized in the usual way [1] so as to yield an estimate of the largest (short-time) Lyapunov exponent for the orbit segment. Configuration space data, recorded at fixed intervals δt, were used to generate a time series $\{K_j(n\,\delta t)\}$ for each of the segments in the 1000 orbit ensemble that was deemed to be chaotic. δt was typically so chosen that each segment was sampled by 2560 points. Distinctions between regular and chaotic were implemented through the introduction of a threshold value $\chi_{\min}$: if the computed $\chi < \chi_{\min}$ the orbit segments were assumed to be regular. Combining all the orbital data for all the chaotic orbits allowed the computation of the bulk moments $\langle K \rangle$ and δK where, recall, $K = \Delta V$. Binning the combined data into 1000 bins yielded a numerical representation of the distribution $N[K]$.

A discretized representation of the average autocorrelation function $\Gamma(t)$ was computed by selecting a representative ensemble of 5120 initial conditions, evolving each of these into the future for an extended time $T \geqslant 2048$, so as to generate a set of well-mixed ''random'' phase-space points, identifying each of the $N_c \leqslant N$ orbit segments that were chaotic, and, by extending the integrations for an additional time $T' = 1024$, constructing

$$\Gamma(n\,\delta t) = \frac{1}{N_c \langle K^2 \rangle} \sum_{j=1}^{N_c} DK_j(T) DK_j(T + n\,\delta t). \tag{5.1}$$

Here, $DK_j \equiv K_j - \langle K \rangle$, and the quantities $\langle K \rangle$ and $\langle K^2 \rangle$ represent averages computed for all the chaotic orbital data for $T < t < T'$. Ideally, one should compute the autocorrelation time τ using the defining relation

$$\int_0^\infty dt\, \Gamma(t) = \langle K^2 \rangle \tau. \tag{5.2}$$

Given, however, that Γ is typically a rapidly oscillating function (period $\sim t_D$) with an envelope that damps very slowly, such a computation proved unreliable. A seemingly better measure of τ or, at least, of how τ scaled with energy E for fixed potential, was obtained by computing the period $\tau_{\rm osc}$ associated with the oscillations.

Predictions associated with a microcanonical distribution were computed as follows: The microcanonical distribution $\mu \propto \delta_D(H-E)$ implies the configuration-space probability density (4.22); but, given this f, it is straightforward to compute the value of any configuration space function $g(q)$. Numerical representations of the distribution $N[K]$ associated with a microcanonical distribution were computed by (i) dividing the occupied configuration space into a collection of M hypercubes, (ii) deciding randomly whether or not to sample each hypercube, using a weighting $\propto (E-V)^{(D-2)/2}$ as evaluated at a random point in the cube, (iii) in the event that the hypercube was to be sampled, locating a point in the cube at a randomly chosen location, and then (iv) binning the resulting collection of points into 1000 bins.

Granted the assumption of a Gaussian distribution of curvatures, estimates of the Lyapunov exponent χ can be, and were, computed using Eq. (4.16), which does not require the assumption of a microcanonical population. When the assumption of a Gaussian distribution is relaxed, an analytic solution is not possible in general, so that χ was obtained instead from a numerical computation, with the random curvature generated initially by sampling $N[K]$, held constant for the autocorrelation time τ, and then replaced by another, randomly chosen curvature [17].

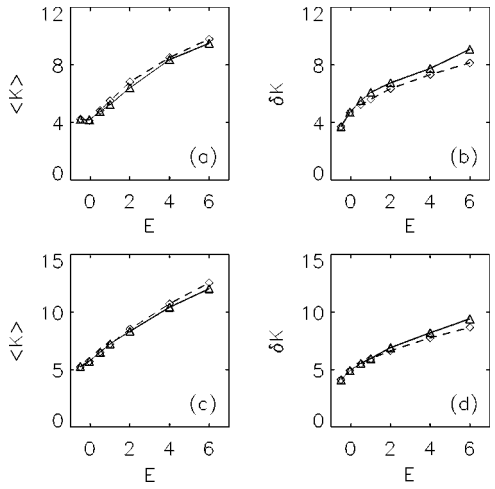

FIG. 4. (a) The mean curvature $\langle K \rangle$ for chaotic orbits in the $D=2$ dihedral potential as a function of energy E, computed assuming a microcanonical distribution (solid line) and extracted directly from orbital data (dashed line). (b) The associated dispersion δK. (c) $\langle K \rangle$ for $D=3$. (d) δK for $D=3$.

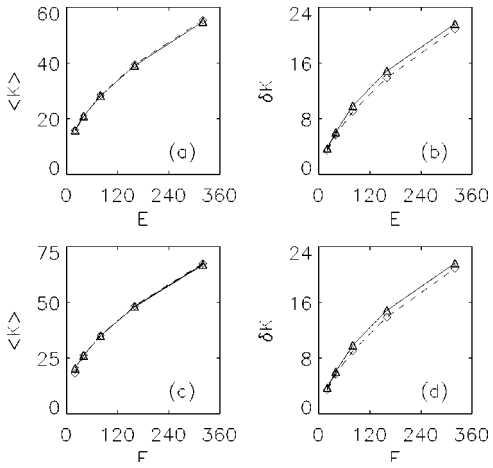

FIG. 5. (a) The mean curvature $\langle K \rangle$ for chaotic orbits in the $D=4$ FPU potential with $a=1.0$ and $b=0.1$ as a function of energy E, computed assuming a microcanonical distribution (solid line) and extracted directly from orbital data (dashed line). (b) The associated dispersion δK. (c) $\langle K \rangle$ for $D=6$. (d) δK for $D=6$.

B. What was found

1. N[K] and its first two moments

Figure 4 exhibits the energy-dependence of the quantities $\langle K \rangle$ and δK for chaotic orbits in the dihedral potential with $D=2$ and 3, computed both from time-series data (dashed lines) and assuming a microcanonical distribution (solid lines). Overall, one observes excellent agreement between the numerical and analytic predictions, particularly for the first moment $\langle K \rangle$. The best overall agreement obtains for lower energies where, even for $D=2$, the measure of regular orbits is comparatively small and ''stickiness'' seems comparatively unimportant.

For $D=2$ at higher energies, say $E>1.0$ or so, it appears that a third of the constant energy hypersurface, or even more, corresponds to regular orbits, so that one is clearly *not* justified in assuming a microcanonical distribution. However, it is evident that the predictions based on a microcanonical distribution remain quite good. That this should be the case is not really surprising. Presuming that the regular islands are not concentrated preferentially at regions where ΔV is especially large or small, it would seem reasonable to assume that, in a sufficiently coarse-grained sense, chaotic orbits still go ''all over'' the energetically allowed regions of configuration space. To the extent, however, that this be true, one might expect moments approximating the moments appropriate for a microcanonical distribution which, for $D=2$, implies [cf. Eq. (4.21)] a uniform configuration space density. Figure 5 exhibits analogous data for the FPU potential with $D=4$ and 6, generated for parameter values $a=1.0$ and $b=0.1$.

The thick solid curves in panels (a)–(d) of Fig. 6 exhibit distributions of curvatures, $N[K]$, for the dihedral potential with $D=2$ and 6 generated assuming a microcanonical distribution. The corresponding curves in Fig. 7 exhibit analogous distributions for the FPU potential for $D=4$ and 6. Panels (e) and (f) in Fig. 6 show the time series and micro-

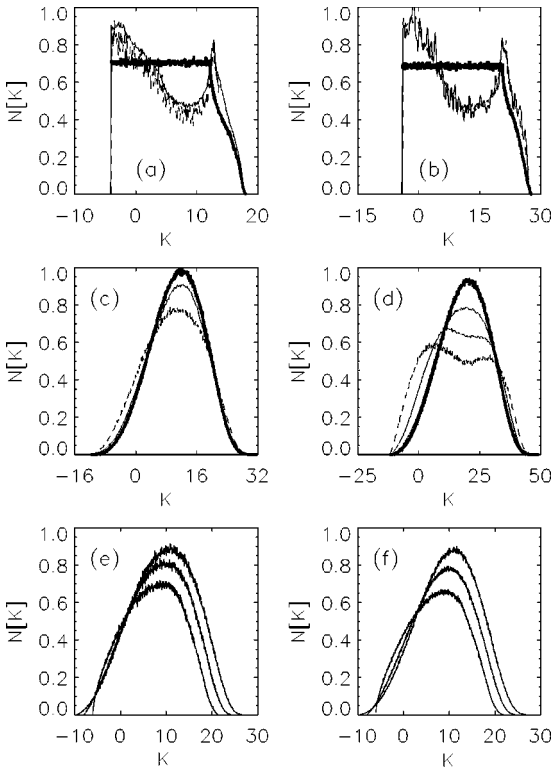

FIG. 6. (a) The distribution of curvatures, $N[K]$, for chaotic orbits with energy $E=1.0$ in the $D=2$ dihedral potential, computed assuming a microcanonical distribution (thick-solid line) and from orbital data for an ensemble evolved for times $t=1024$ and 3172. (b) $N[K]$ for $D=2$ and $E=6.0$. (c) $N[K]$ for $D=6$ and $E=1.0$. (d) $N[K]$ for $D=6$ and $E=6.0$. (e) $N[K]$, as generated from time-series data for $t=3172$, for $E=1.0$ with $D=3$, $D=4$, and $D=5$. (f) $N[K]$ for $E=1.0$ with $D=3$, $D=4$, and $D=5$, now generated assuming a microcanonical distribution.

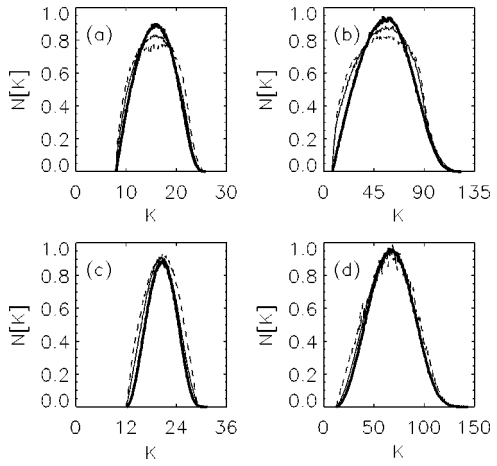

FIG. 7. (a) The distribution of curvatures, $N[K]$, for chaotic orbits with energy $E=20$ in the $D=4$ FPU potential with $a=1.0$ and $b=0.1$, computed assuming a microcanonical distribution (thick-solid line) and from orbital data for an ensemble evolved for times $t=1024$ and 4196. (b) $N[K]$ for $D=4$ and $E=320$. (c) $N[K]$ for $D=6$ and $E=20$. (d) $N[K]$ for $D=6$ and $E=320$.

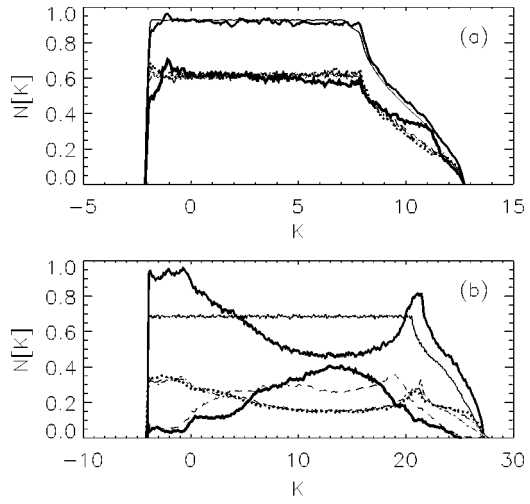

FIG. 8. (a) The distribution of curvatures, $N[K]$, for a representative ensemble of 1000 orbits with energy $E=-0.5$ in the $D=2$ dihedral potential. The five lower curves represent subdistributions, generated by dividing the ensemble into five quintiles based on the values of the short-time Lyapunov exponents for the orbits. The near-horizontal upper curve represents the distribution $N[K]$ predicted by a microcanonical distribution; the other, more jagged upper curve represents the distribution $N[K]$ associated with the full 1000 orbit ensemble, given by the sum of the five lower curves. (b) The same for $E=6.0$.

canonical predictions for the dihedral potential in (from left to right) $D=3$, 4, and 5. It is evident that the microcanonical distributions for the dihedral potential with $D=2$ are not even remotely Gaussian in shape. However, it is also apparent that, for all the other cases, the distribution is in fact reasonably well fit by a Gaussian, although $N[K]$ typically has a slight skew and can manifest appreciable deviations for large $|K-\langle K\rangle|$.

The other curves in Figs. 6(a)–6(d) and in Fig. 7 represent distributions $N[K]$ generated from time-series data. Figure 7 and the first three panels of Fig. 6 display two numerical curves, one representing data for $0<t<1024$ and the other for $2048<t<3072$. Figure 6(d) also includes a third numerical curve, generated for $8192<t<9216$. For the two energies exhibited in the $D=2$ dihedral potential, $E=1.0$ and 6.0, there exist large measures of both regular and chaotic orbits and, for this reason, the time-series $N[K]$ differs significantly from the microcanonical $N[K]$. However, the ensembles of initial conditions used to generate the time-series distributions evolved towards an invariant (albeit nonmicrocanonical) distribution relatively quickly, so that the two numerical curves very nearly overlap.

For the dihedral potential with $D\geqslant 3$ and for the FPU potential with $D\geqslant 4$, almost all the orbits appear to be chaotic, so that, assuming ergodicity, the microcanonical $N[K]$ and a truly representative time-series $N[K]$ should coincide up to statistical uncertainties. However, for the cases exhibited in Figs. 6(c) and 6(d) and Fig. 7, the initial ensembles only converged towards an invariant distribution on a comparatively long time scale, so that the two (or more) time-series curves differ appreciably from one another. In each case, the later time sampling(s) yielded distributions $N[K]$ that more closely approximated the microcanonical $N[K]$.

The preceding suggests that one may use the form of the distribution $N[K]$ as a robust diagnostic in terms of which to probe the approach towards ergodicity. Ergodicity *per se* is an assumption regarding the $t\rightarrow\infty$ limit and, even assuming ergodicity, there remains an obvious question: How long must one evolve some ensemble of initial conditions before its time-averaged density closely approximates the density associated with a constant population of the accessible phase space regions? Comparing the distribution $N[K]$ associated with an evolving ensemble with the $N[K]$ associated with a microcanonical distribution can provide a useful diagnostic for probing the extent to which the ensemble has evolved towards a time-independent invariant distribution.

It is well known that different chaotic orbit segments in the same connected phase-space region can exhibit vastly different short-time Lyapunov exponents, and that the values of these short-time exponents may correlate significantly with position. For example, chaotic segments near regular islands tend to be much less unstable than wildly chaotic segments located in the middle of the stochastic sea. One might, therefore, expect that orbit segments with especially large or small short-time exponents would be characterized by different curvatures. For potentials and energies where almost all the orbits are chaotic and ''stickiness'' is rare, this segregation should be minimal; but for potentials where there is a coexistence of large measures of both regular and chaotic orbits, and where ''stickiness'' is pronounced, this effect should be much more pronounced.

As illustrated in Fig. 8, this intuition was corroborated numerically. The top panel of Fig. 8 was generated for $E=-0.5$ in the $D=2$ dihedral potential, an energy where the regular regions are extremely small, so that a representative ensemble of 1000 initial conditions, integrated for a time $T=1024$, yielded no regular orbits. The orbits generated from these initial conditions were divided into five quintiles, depending on the values of their short-time Lyapunov expo-

nents, and the lower-five curves in this panel exhibit individual subdistributions $N[K]$ computed for each quintile. The four quintiles corresponding to the larger values of χ yielded distributions that were nearly identical. The lowest quintile was again quite similar, but did manifest some noticeable differences: This subdistribution, corresponding to the thick-solid line, is distinctly underrepresented at very low values of K and over represented at very large K, and, unlike the other four quintiles, appears to be a slowly decreasing function of K in the interval $0<K<7.5$. The sum of these five subdistributions (with a different normalization from the subdistributions) corresponds to the slightly jagged upper curve, which is essentially identical, modulo statistical uncertainties, to the smoother curve computed for a microcanonical distribution.

The lower panel of Fig. 8 exhibits analogous data for $E=6.0$, again in the $D=2$ dihedral potential. In this case, a 1000 orbit ensemble was divided instead into a ''quintile'' of 332 regular orbits and four''quintiles'' each comprised of 167 chaotic orbits, but the resulting subensembles were analyzed identically. The lower solid curve peaking at $K\sim 13$ represents the 332 regular orbits, and the three nearly identical curves that have a local minimum at $K\sim 13$ correspond to the chaotic orbit segments with the largest short-time Lyapunov exponents. The intermediate dashed curve corresponds to the chaotic orbits with the smallest short-time Lyapunov exponent, the majority of which could be reasonably classified as ''sticky.'' The total $N[K]$ given as a sum of the four chaotic ''quintiles'' is represented by the upper curve with a local minimum at $K\sim 13$. The upper curve corresponding to a nearly flat profile again corresponds to a microcanonical distribution.

2. The autocorrelation time τ

As suggested by Casetti *et al.*, the autocorrelation function $\Gamma(t)$ is in fact an oscillating function of time, but it tends to decay more slowly than with the $1/t$ envelope implicit in Eq. (4.14). This slower decay is especially evident for potentials and energies when ''stickiness'' is important, in which case a substantial ''memory'' may persist for dozens of oscillations. This is, e.g., evident in Figs. 9(a)–9(d), which exhibit data for the dihedral potential for $D=2$ and 6. The first two panels correspond to a very low-energy $E=-0.5$, where, even for $D=2$, almost all the orbits are chaotic. The second two panels correspond to a higher-energy $E=6.0$ where, for both $D=2$ and 6, chaotic segments can be nearly periodic and have comparatively small short-time Lyapunov exponents. For $D=2$, the case exhibited in panel (c), roughly one quarter of the chaotic orbits are noticeably ''sticky,'' for $D=6$, the case in panel (d), the fraction is reduced to about 5%. In either case, analysis of a sample that excludes ''sticky'' segments yields an autocorrelation function that decays substantially more quickly.

As noted by Casetti *et al.*, if the autocorrelation function is in fact well approximated by Eq. (4.13) the time scale identified geometrically in Eq. (4.12) should coincide with the time scale (4.14). This prediction was tested numerically and found typically to be satisfied to within factors of ~ 2, although some discrepancies were observed. As noted already, a direct determination of τ using Eq. (5.2) proved unreliable.

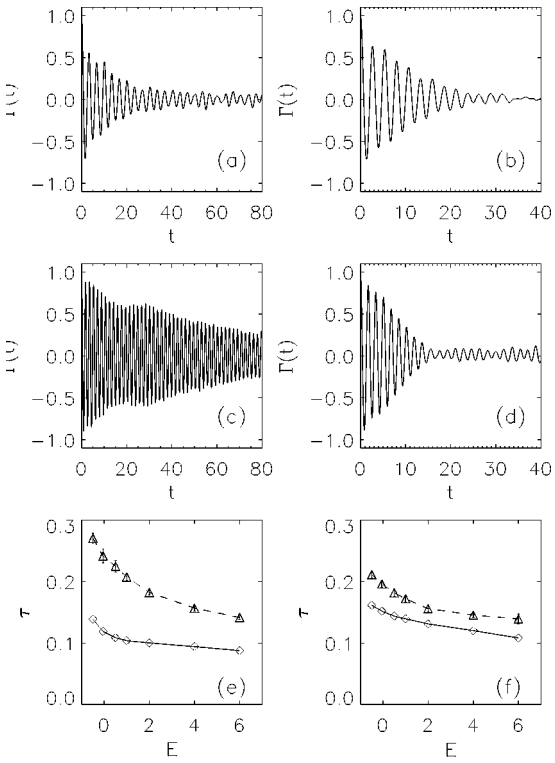

FIG. 9. (a) The autocorrelation function $\Gamma(t)$ for chaotic orbits in the $D=2$ dihedral potential with $E=-0.5$. (b) The same for $D=6$ and $E=-0.5$. (c) The same for $D=2$ and $E=6.0$. (c) The same for $D=6$ and $E=6.0$. (e) The Casetti *et al.* time scale τ of Eq. (4.12) (solid line) and the time scale $\tau_{\rm osc}/4\pi$ of Eq. (4.14) (dashed line), for chaotic orbits in the $D=2$ dihedral potential at different energies E. (f) The same for $D=6$.

Perhaps the most striking point is that, at least when ''stickiness'' is comparatively unimportant, the Casetti *et al.* time scale τ given by Eq. (4.13) and the time scale $\tau_{\rm osc}$ exhibit very similar scaling with energy E. This is illustrated in Figs. 9(e) and 9(f), which exhibit both time scales as functions of E for the $D=2$ and 6 dihedral potential. In each case, the time scale $\tau_{\rm osc}$ is somewhat longer than the Casetti *et al.* time scale τ. Significantly, though, for $D=2$, the quantities $\tau_{\rm osc}$ and τ exhibit very different scalings at higher energies, precisely where ''stickiness'' is most prominent.

3. Sources of uncertainty

Granted the assumption of a Gaussian distribution of curvatures, the predicted value of the largest Lyapunov exponent depends on only three quantities, namely $\langle K\rangle$, δK, and τ; and as such, it is natural to ask how the predicted value $\chi_{\rm est}$ varies if any of these inputs are changed.

If one introduces a simultaneous scaling of both $\langle K\rangle$ and δK, i.e., $\langle K\rangle\to\alpha\langle K\rangle$ *and* $\delta K\to\alpha\,\delta K$, with α of order unity, $\chi_{\rm est}\to\alpha^{1/2}\chi_{\rm est}$. If, alternatively, $\langle K\rangle$ is held fixed but $\delta K\to\alpha\,\delta K$, one infers, at least approximately, that $\chi_{\rm est}\to\alpha^{3/2}\chi_{\rm est}$. Finally, if $\langle K\rangle$ and δK are held fixed, but one allows for a scaling $\tau\to\alpha\tau,\chi_{\rm est}\to\alpha\chi_{\rm est}$.

Given that the values of $\langle K \rangle$ and δK can be estimated quite well using simple dimensional arguments—recall that, even when there are relatively large measures of periodic orbits, a microcanonical population yields estimates in good agreement with the results of direct numerical computation—it would seem that, with the assumption of quasi-isotropy and a Gaussian distribution of curvatures, the largest source of error should be in the determination of the autocorrelation time τ. The expression for τ motivated by Casetti *et al.* is more *ad hoc* than the expression for $\langle K \rangle$ and δK; and dimensional arguments are hard pressed to yield estimates of τ that are accurate to better than a factor of two. However, factors of two uncertainty in τ translate directly into factors of two uncertainty in $\chi_{\rm est}$.

One may also investigate how the predicted $\chi_{\rm est}$ changes if one relaxes the assumption of a Gaussian distribution, instead computing $\chi_{\rm est}$ by solving Eq. (4.9) numerically for the distribution $N[K]$ generated either from a microcanonical distribution or from real orbital data. The resulting change in $\chi_{\rm est}$ will of course depend on the degree to which $N[K]$ deviates from a Gaussian, larger deviations resulting in larger changes. Especially for two-dimensional systems, where $N[K]$ is far from Gaussian, allowing for the correct distribution may change $\chi_{\rm est}$ by a factor of three, or even more.

This is illustrated in Fig. 10, which exhibits several different estimates of the largest Lyapunov exponents $\chi_{\rm est}$ for the $D=2$ dihedral potential, most of which will be described in Sec. VI. In the present context, note simply (i) the ''true'' $\chi_{\rm num}$, generated by tracking a small initial perturbation (solid line), (ii) the Casetti *et al.* $\chi_{\rm est}$, based on the assumption of Gaussian fluctuations and an autocorrelation time given by Eq. (4.13) (short dashes); and (iii) an alternative $\chi_{\rm est}$, again based on the ''quasi-isotropized'' Eq. (4.9), but now allowing for a distribution $N[K]$ generated from time-series data and an autocorrelation time (4.15) (long dashes). Both estimates are comparable in magnitude to $\chi_{\rm num}$, but both miss the nontrivial dip that arises near $E=0.0$.

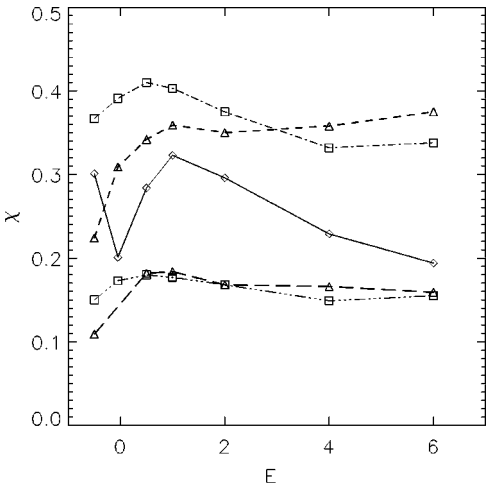

FIG. 10. Estimated values of the largest Lyapunov exponent for the $D=2$ dihedral potential as a function of energy: $\chi_{\rm num}$ generated from direct numerical integration (solid curve), the Casetti *et al.* value, generated assuming a Gaussian $N[K]$ and autocorrelation time τ given by Eq. (4.12) (short dashes); an estimate based on Eq. (4.8), but now using the $N[K]$ generated from a time-series analysis and τ given by Eq. (4.14) (long dashes); an estimate based on Eq. (6.6), using ω_- and τ given by Eq. (4.14) (dot dashes); and an estimate based on the coupled oscillator system, assuming Gaussian fluctuations and τ given by Eq. (4.12).

Figure 11 compares the numerical and estimated $\chi(E)$ for the dihedral potential for $D=2$, 3, 4, and 6. The estimated values were computed using Eq. (4.13), based on a Gaussian distribution, with moments generated both from a time-series analysis (dashed lines) and assuming a microcanonical distribution (dotted lines). The numerical values are connected with a solid line. One observes significant differences in the shapes of the curves associated with the numerical and estimated values, but there is invariably an overall agreement to within a factor of two. The most striking discrepancies arise for $D=2$, where the estimates completely miss the abrupt dip

VI. ESTIMATES OF LYAPUNOV EXPONENTS IN LOWER-DIMENSIONAL HAMILTONIAN SYSTEMS

A. Estimates of the true Lyapunov exponent

Overall, Eq. (4.15) first proposed by Casetti *et al.*, modified to allow for moments computed assuming a microcanonical distribution, appears to give reasonable estimates of the largest Lyapunov exponent in lower-dimensional Hamiltonian systems, provided that an appreciable fraction of the phase space corresponds to chaotic orbits. In particular, as long as the true Lyapunov exponents are not very small ($\chi_{\rm num} \ll t_D^{-1}$) and/or ''stickiness'' is not especially prominent, the estimated $\chi_{\rm est}$ typically agree with the numerical $\chi_{\rm num}$ to within factors of two. In some cases, such as for the FPU model, the agreement between $\chi_{\rm num}$ and $\chi_{\rm est}$ rapidly increases with increasing D; but in other cases, such as for the dihedral potential, this is *not* the case. This would suggest that the quasi-isotropy assumption, which should become increasingly justified in higher dimensions, is *not* necessarily the principal source of error.

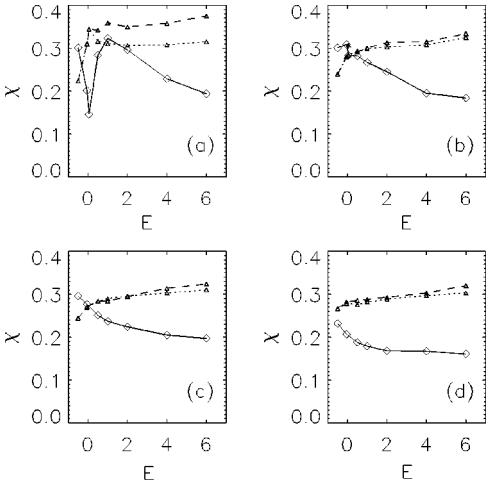

FIG. 11. Estimated values of Lyapunov exponents for orbits in the dihedral potential, generated from numerical integrations (solid lines) and estimated using Eq. (4.12). (a) For $D=2$. (b) $D=3$. (c) $D=4$. (d) $D=6$.

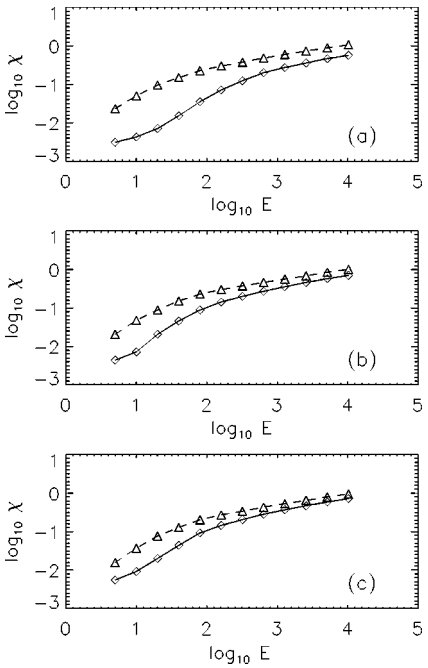

FIG. 12. Estimated values of Lyapunov exponents for orbits in the FPU model, generated from numerical integrations (solid lines) and estimated using Eq. (4.12). (a) For $D=4$. (b) $D=5$. (c) $D=6$.

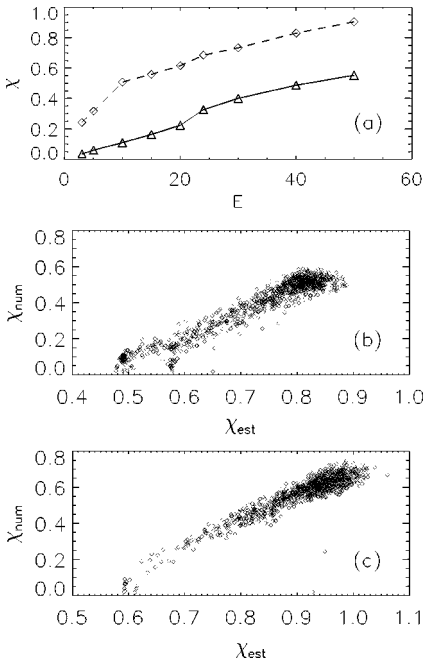

FIG. 13. (a) Estimated values of Lyapunov exponents for orbits in the truncated Toda potential, generated from numerical integrations (solid lines) and estimated using Eq. (4.12). (b) Short-time Lyapunov exponents computed using Eq. (4.12) ($\chi_{\rm est}$) and generated from numerical integrations ($\chi_{\rm num}$) for $E=30.0$. (c) The same for $E=50.0$.

in $\chi_{\rm num}$ for $E\sim 0$. The fact that, for $D=2$, the two estimated curves differ significantly at high energies reflects the fact that the constant energy hypersurface contains large regular islands, so that the invariant distribution is far from microcanonical.

Figure 12 exhibits the numerical and estimated $\chi(E)$ for the FPU model for $D=4$, 5, and 6, with the estimated values again computed assuming Gaussian distributions and moments generated from a time-series analysis. The data have been plotted on a log-log plot to facilitate comparison with Fig. 3 in Casetti *et al.* Here, two points are immediately obvious: (1) The estimated and numerical curves are distinctly different, with $\chi_{\rm est}$ always larger than $\chi_{\rm num}$, but their curvatures are comparatively similar. (2) The agreement between $\chi_{\rm num}$ and $\chi_{\rm est}$ becomes progressively better for higher dimensions and for higher energies. For $E=5$ in $D=4$, where the numerical $\chi_{\rm num}=0.211$ corresponds to a very long time $t\sim 45\gg t_D$, $\chi_{\rm est}$ overestimates $\chi_{\rm num}$ by nearly a factor of seven. For $D=6$ and $E=5$, $\chi_{\rm est}$ yields a value approximately 2.65 times too large; for $E=10\,240$, its value is only 1.27 times too large.

Figure 13(a) exhibits the same data for the sixth-order truncation of the Toda potential. As for the FPU model, $\chi_{\rm est}$ systematically overestimates the true $\chi_{\rm num}$, the largest errors arising at low energies, where $\chi_{\rm num}$ is comparatively small, larger regular islands exist, and ''stickiness'' is especially important.

B. Short-time Lyapunov exponents

The computations described in the preceding subsection indicate that, for a variety of lower-dimensional systems, the Casetti *et al.* model of a stochastic-oscillator equation yields reasonable estimates of the largest Lyapunov exponent χ as a function of energy E. However, if the stochastic-oscillator picture is to be accepted as completely valid, one must also demand that it ''explain'' the varying degrees of chaos manifested by different chaotic orbit segments with the same energy, as probed by short-time Lyapunov exponents. In particular, one might hope that, even if the estimated values $\chi_{\rm est}$ of the true Lyapunov exponent disagree significantly with the values $\chi_{\rm num}$ computed numerically, the estimated and computed values of short-time Lyapunov exponents for different orbit segments with the same energy should be strongly correlated. For example, chaotic segments for which the true short-time $\chi_{\rm num}$ is especially small should yield estimates $\chi_{\rm est}$ that are also especially small.

That such correlations do in fact exist is illustrated in Figs. 13(b) and 13(c) and Fig. 14, which exhibit results appropriate for, respectively, the truncated Toda and dihedral potentials. Each of these figures was generated by (i) selecting a representative ensemble of 1000 initial conditions, all with the same energy; (ii) evolving these into the future for a time $T=1024$ while simultaneously tracking the evolution of a small perturbation so as to generate $\chi_{\rm num}$; (iii) recording the values of K for each orbit at fixed intervals $\delta t=0.4$; (iv) analyzing each orbit to extract $\langle K\rangle$ and δK; and (v) using these two moments along with Eq. (4.13) to generate an estimated $\chi_{\rm est}$. The scatter plots provide unambiguous visual confirmation that the values of $\chi_{\rm num}$ and $\chi_{\rm est}$ are strongly correlated.

This visual impression may be quantified by computing the Spearman rank correlation $\mathcal{R}$ between the values of $\chi_{\rm est}$

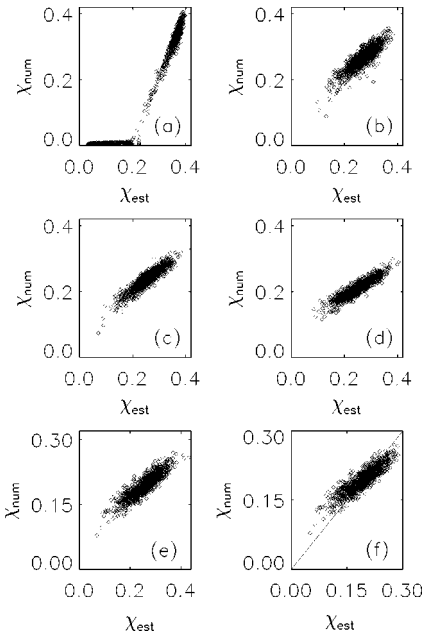

FIG. 14. (a) Short-time Lyapunov exponents computed using Eq. (4.12) (χ_{est}) and generated from numerical integrations (χ_{num}) for $E=1.0$ in the $D=2$ dihedral potential. (b) The same for $D=3$. (c) $D=4$. (d) $D=5$. (e) $D=6$. (f) χ_{num} for $D=6$ contrasted with revised estimates χ_{est} generated by rescaling the time scale τ of Eq. (4.12) by a factor of 0.75.

and χ_{num} in each ensemble, which satisfies

$$\mathcal{R}(\chi_{num},\chi_{est})=1-\frac{6}{N^3-N}\sum_{i=1}^{N}\delta_i^2. \tag{6.1}$$

Here $N=1000$ denotes the number of orbits in the ensemble and δ_i denotes the difference in rank for the ith orbit when ordered in terms of χ_{num} and χ_{est}. $\mathcal{R}=1$ corresponds to a perfect correlation; $\mathcal{R}=-1.0$ corresponds to a complete anti-correlation.

The data sets in Figs. 13(b) and 13(c), corresponding to $E=30$ and 50 in the truncated Toda potential, both yield $\mathcal{R}\approx 0.88$. The data sets in Figs. 14(a)–14(e), corresponding to $E=1.0$ in the dihedral potential, yield rank correlations ranging between a low of $\mathcal{R}\approx 0.85$ for $D=3$ and a high of $\mathcal{R}\approx 0.95$ for $D=2$. The especially high-rank correlation for $D=2$ might seem surprising since the ensemble contains a large number of regular orbit segments, with very small χ_{num}. The reason $\mathcal{R}$ remains as large as it does is that, for orbit segments that are manifestly regular, so the χ_{num} eventually decays to zero, there is a correlation between the estimated value χ_{est} and the rate at which χ_{num} tends to zero: for regular orbits where the short-time χ_{est} is especially large, the convergence is especially slow, so that, at finite times, χ_{num} will also be especially large [18].

Not surprisingly, the computed value of $\mathcal{R}$ for a given ensemble of initial conditions depends on the total integration time. If the orbits be integrated for a sufficiently large T, their differences tend to ''wash out,'' so that the observed range of values for χ_{num} and χ_{est} both decrease. Eventually, the differences between different orbit segments become small and the pronounced correlation disappears.

It would seem visually from Figs. 14(a)–14(e) that the numerical and estimated values of the short-time Lyapunov exponents deviate largely because of some overall scaling. Given that at least for $D\geqslant 3$, the phase space is almost entirely chaotic, so that the distribution of curvatures reflects a microcanonical distribution, the evidence (cf. Fig. 6) that this implies a nearly Gaussian distribution, and the argument in the preceding subsection that quasi-isotropy is not necessarily the principal source of discrepancies, it would seem natural to conjecture that this reflects a misidentification of the proper autocorrelation time τ. Panel (f) in Fig. 14 shows what happens to the estimated value χ_{est} for the $D=6$ dihedral potential if, for each orbit, τ is reduced by a factor of ≈ 0.75, the value required to ensure that, for the ensemble, the mean values of the estimated and numerical exponents coincide, i.e., $\langle\chi_{est}\rangle=\langle\chi_{num}\rangle$. The net result is that, to a fair degree of approximation, the data points are aligned along $\chi_{est}=\chi_{num}$.

C. The special case $D=2$

It is natural to ask whether one can relax the assumption of quasi-isotropy, at least for $D=2$, where it would seem most suspect. One way in which to do this would be to work instead with the Jacobi metric, which, for $D=2$, leads to a single oscillator equation of the form [7,19]

$$\frac{d^2\xi}{dt^2}-\frac{1}{W}\frac{dW}{dt}\frac{d\xi}{dt}+\tilde{K}\xi=0, \tag{6.2}$$

where $W=E-V(q^i)$ denotes the kinetic energy and

$$\tilde{K}=\Delta V+\frac{1}{W}|\nabla V|^2. \tag{6.3}$$

Unfortunately, however, this equation is very difficult to explore numerically since it yields near-divergences for $W\approx 0$, which prove quite common for $D=2$.

Alternatively, within the setting discussed hitherto in this paper, there are two ways in which one might proceed:

(1) Consider the full multidimensional Jacobi equation and view it as a matrix stochastic equation. This could at least provide the ''average'' rate of exponential instability in different configuration space directions. Quite generally, a small perturbation ξ^i will satisfy

$$\frac{d^2\xi^i}{dt^2}+\sum_j V_{ij}\xi^j=0, \tag{6.4}$$

with $V_{ij}\equiv\partial^2 V/\partial q^i\partial q^j$ the second derivative matrix. The objective then is to view each component of this matrix as an (approximately) independent stochastic variable, i.e., considering

$$V_{ij}=V_{ji}=\Omega_{0,ij}+\delta\Omega_{ij}, \tag{6.5}$$

with $\delta\Omega_{ij}$ a random variable. Given distributions $N[V_{xx}]$, $N[V_{yy}]$, and $N[V_{xy}]=N[V_{yx}]$, which can be computed from time-series data or assuming ergodicity, and some approximation to the autocorrelation functions Γ_{xx}, Γ_{yy}, and Γ_{xy}, which may again be motivated either from a time series or assuming ergodicity, this system is easy to solve numerically [20].

(2) At least for $D=2$, it is easy to diagonalize the matrix Eq. (4.2) at any given instant so as to obtain the eigenvalues of the stability matrix. The corresponding eigenvectors will then satisfy equations of the form

$$\frac{d^2\xi_\pm}{dt^2}+\omega_\pm\xi_\pm=0, \tag{6.6}$$

where the time-independent eigenvalues satisfy

$$\omega_\pm=\tfrac{1}{2}(V_{xx}+V_{yy})\pm\tfrac{1}{2}[(V_{xx}-V_{yy})^2+4V_{xy}^2]^{1/2}. \tag{6.7}$$

Viewing $\omega_\pm=\Omega_{0,\pm}+\delta\Omega_\pm$ as stochastic variables leads to a pair of decoupled-oscillator equations that are easy to solve numerically. In general, one might anticipate that the smaller eigenvalue will correspond to the more rapid growth rate.

These alternatives were tested in detail for the $D=2$ dihedral potential. The principal results are summarized in Fig. 10, which shows the numerical $\chi_{\rm num}(E)$ (solid line) as well as estimated values $\chi_{\rm est}(E)$ generated in four different ways. The short- and long-dashed lines, discussed already in the preceding section, correspond to the isotropized Eq. (4.9), assuming a microcanonical distribution (short dashes) or using inputs generated from orbital data (long dashes). The triple-dot-dashed curve represents the values generated for the coupled-oscillator system and the dot-dashed curve represents the values generated by solving Eq. (6.6) for ω_-. All the estimated curves yield values $\chi_{\rm est}$ that agree with $\chi_{\rm num}$ to within factor of two, but none seems especially better than the others.

The hypothesis that chaotic behavior in lower-dimensional Hamiltonian systems may be modeled by a stochastic-oscillator equation would appear robust in the sense that different implementations all lead to predictions that yield at least rough agreement with numerical integrations. However, none of the alternatives considered here would appear ''completely right.'' It seems likely that, in very low-dimensional systems, the details matter sufficiently that no universal prescription will yield a completely accurate prediction.

VII. CONCLUSIONS AND DISCUSSION

The results described in this paper strongly corroborate the intuition that chaotic motion in lower-dimensional Hamiltonian systems may be visualized as random, so that the average instability of chaotic orbits, and hence, the values of their largest Lyapunov exponents, can be derived from a harmonic-oscillator equation with a randomly varying frequency. Modulo straightforward modifications, technical rather than conceptual in nature, the approach introduced by Casetti *et al.* for higher-dimensional systems also works reasonably well for systems with dimensionality as low as $D=2$. In this sense, as suggested in the Introduction, one would appear to have a clear alternative paradigm in terms of which to interpret the origins of chaos in lower-dimensional Hamiltonian systems.

The precise numerical values of χ predicted using this analytic approach are somewhat less accurate in lower dimensions than they are for much larger D, but it remains true that, in general, this approach yields predictions that are correct to within a factor of two. In principle, one might hope to do still better but, as a practical matter, this would seem difficult if not impossible. The ''obvious'' alternatives considered in Sec. VI C yield somewhat different predictions for the largest Lyapunov exponents. In some cases, these predictions are somewhat better than those based on Eqs. (4.12), (4.15), and (4.16) but, overall, they seem neither appreciably better nor appreciably worse. This would suggest that the predictions based on these equations are comparatively robust, in the sense that minor modifications do not yield vastly different results. However, this might also suggest that there is no single, universal modification that one might introduce that would yield near-perfect agreement for all potentials and energies. In point of fact, this is hardly surprising. There is every reason to expect that details that should ''wash out'' in higher-dimensional systems will remain important in lower-dimensional systems. A ''thermodynamic'' description of chaos should work best for systems with many degrees of freedom.

In this context, two significant points should be stressed.

(1) Even when the predicted values $\chi_{\rm est}(E)$ of the ''true'' Lyapunov exponent $\chi_{\rm num}(E)$ are off by as much as a factor of two, one observes strong correlations between $\chi_{\rm est}(E)$ and $\chi_{\rm num}(E)$ for different orbit segments with the same energy. Orbit segments for which the predicted $\chi_{\rm est}$ is low tend to have small short-time exponents $\chi_{\rm num}$; and, similarly, segments for which $\chi_{\rm est}$ is high tend to have larger values of $\chi_{\rm num}$. The physics entering into Eqs. (4.12), (4.15), and (4.16) allow one to distinguish clearly between orbit segments that are ''wildly chaotic'' in visual appearance and have especially large short-time exponents and ''sticky'' segments that are nearly regular in appearance and have comparatively small short-time exponents.

(2) The largest discrepancies between the predicted and numerically computed Lyapunov exponents occur invariably for those potentials and energies where large portions of the chaotic sea correspond to ''sticky'' orbits manifesting nearly regular behavior, in which case $\chi_{\rm est}$ can be much larger than the ''true'' $\chi_{\rm num}$. This is exactly what one would expect. If large portions of the stochastic sea are ''sticky,'' an orbit will spend much of its time evolving in a nearly regular fashion, but it is clear that, while manifesting such near-regular behavior, its motion cannot be characterized as essentially random. Indeed, as discussed more carefully elsewhere [7], chaotic orbit segments for which $\langle K\rangle$ and δK assume values close to those characteristic of regular orbits tend systematically to have very small short-time Lyapunov exponents.

The principal difference between the approach developed in this paper and the approach introduced by Casetti *et al.* is that the statistical properties of the mean curvature K are not

derived assuming a canonical distribution. For a truly conservative system, a thermodynamic description must, strictly speaking, be based on a microcanonical distribution, and it is only for large D that one can approximate such a ''correct'' description by a description based on a canonical distribution. Moreover, for very low dimensions, especially $D=2$, even a microcanonical distribution is clearly unjustified. A microcanonical analysis is based on the assumption that the entire constant-energy hypersurface is chaotic, but for lower dimensions, nonintegrable systems typically exhibit a coexistence of regular and chaotic regions, both with significant measure. A correct analysis must involve deriving the statistics of the curvature only in the chaotic phase-space regions, a task that seems difficult analytically but, given an assumption of ergodicity, is straightforward to implement via a time-series analysis.

In part, this work concerning chaos and the phase mixing of chaotic orbits was motivated in the context of nonequilibrium systems comprised of a large number of interacting particles. Examples of such systems include self-gravitating systems, e.g., galaxies, and charged-particle beams governed by external focusing forces and internal Coulomb forces (space charge). For both these examples, fast evolutionary time scales have profound consequences. For galaxies, they are an integral part of the formation process [21]. For beams, they limit the degree to which an accelerator designer may preserve the beam quality, especially insofar as the evolution is irreversible [22].

As mentioned in Sec. II, one way to infer the fastest time scale is to consider the interaction of a single particle with the coarse-grained potential formed by all the other particles. The problem then reduces to one involving a low-dimensional Hamiltonian, and the obvious question is to what extent statistical arguments concerning the behavior of chaotic single-particle orbits may be invoked to simplify the analysis further. All the examples presented herein suggest that time scales in low-dimensional Hamiltonian systems inferred via the statistical methods of Casetti *et al.* are typically valid within a factor of order two. They also suggest that uncertainties in the computation of these time scales are principally associated with uncertainties in the autocorrelation time, and that these time scales are comparatively insensitive to the choice of the invariant measure that weights the statistical averages. More importantly, however, our examples reinforce the idea advanced by Cerruti-Sola and Pettini [23] that rapid mixing originates from parametric instability due to positive-curvature fluctuations along the geodesic trajectories of the particles over the configuration-space manifold. Cerruti-Sola and Pettini conjectured that, ''This mechanism is apparently the most relevant—and in many cases unique—source of chaoticity in physically meaningful Hamiltonians.'' The diverse set of examples presented here would seem to corroborate their conjecture.

The statistical analysis, however, does carry some *caveats*. It generally ''predicts'' fast exponential mixing in potentials that are known *a priori* to be integrable and thereby admit only regular orbits that can only mix secularly. Examples include spherically symmetric potentials for which Poisson's equation generates nonuniform density distributions, and special triaxial potentials such as the Staeckel potentials [24]. Thus, the analysis provides no information as to what criteria are necessary and sufficient to establish a preponderance of globally chaotic orbits; it merely hypothesizes their existence. Related to this deficiency is the failure of the analysis to account for ''sticky'' chaotic orbit segments that, when present, will tend to slow down the mixing. Real systems may, however, mitigate these *caveats*. For example, external noise, even with very small amplitude, is known to add greatly to the efficiency of chaotic mixing by overcoming ''stickiness'' [25]. And the presence of localized irregularities that have been coarse-grained away may increase the chaoticity of the orbits. An important point, however, is that the graininess that manifests itself in binary particle interactions is *not* necessarily an example of such localized irregularities. Graininess establishes diffusion of an orbit away from the trajectory it would have in the smooth potential but, at least for nonchaotic orbits, this diffusion involves a secular, rather than exponential, divergence of trajectories [26].

Because it is based on the Eisenhart metric, the present treatment is restricted to stationary systems. However, with a Finsler metric, the geometric method may also incorporate potentials that are explicitly time dependent and/or velocity dependent [27]. For example, recent work involving the Hénon-Heiles potential [28] resulted in a geometric measure of chaos over the associated Finsler manifold that was used for fast computation of the system's Poincaré surface of section. If used with a coarse-grained potential, the Eisenhart metric includes no mechanism for changing the particle energies. In principle, it may be included with a Finsler metric based on a time-dependent coarse-grained potential; however, the generalization also requires specifying a suitable invariant measure for the nonequilibrium system [29].

One final point should be noted. In writing this paper, the authors have deliberately adopted a tact somewhat complementary to that adopted by Casetti *et al.* Rather than focusing on the differential geometry of spaces admitting an Eisenhart metric, the discussion has, to the extent possible, been couched in the language of conventional Hamiltonian mechanics. Such an approach serves to make the ideas underlying the general approach more transparent physically and, it is hoped, will make the picture of chaotic motion as a random process comprehensible to a substantially larger audience.

ACKNOWLEDGMENTS

This research was supported in part by NSF Grants Nos. AST-0070809 and AST-0087666, and in part by the Universities Research Association, Inc., under Contract No. DE-AC02-76CH00300 with the U.S. Department of Energy.

[1] See, e.g., A. J. Lichtenberg and M. A. Lieberman, *Regular and Chaotic Dynamics* (Springer, Berlin, 1992).
[2] L. P. Eisenhart, Ann. Math. **30**, 591 (1929).
[3] E. Hopf, Trans. Am. Math. Soc. **39**, 229 (1936).
[4] D. V. Anosov, Trudy Mat. Inst. Steklov **90**, 1 (1967).
[5] M. Pettini, Phys. Rev. E **47**, 828 (1993).
[6] M. Toda, J. Phys. Soc. Jpn. **22**, 431 (1967).
[7] H. E. Kandrup, Phys. Rev. E **56**, 2722 (1997).
[8] L. Casetti, C. Clementi, and M. Pettini, Phys. Rev. E **54**, 5969 (1996).
[9] H. E. Kandrup and I. V. Sideris, Celest. Mech. (to be published).
[10] D. Armbruster, J. Guckenheimer, and S. Kim, Phys. Lett. A **140**, 416 (1989).
[11] Cf., J. Ford, Phys. Rep. **213**, 271 (1992).
[12] Cf., P. Grassberger, P. Badii, and A. Poloti, J. Stat. Phys. **51**, 135 (1988).
[13] Cf., L. D. Landau and E. M. Lifshitz, *Mechanics* (Pergamon, Oxford, 1969), Sec. 44.
[14] N. G. Van Kampen, Phys. Rep. **24**, 71 (1976).
[15] G. Contopoulos, Astrophys. J. **76**, 147 (1971).
[16] Cf., I. V. Pogorelov and H. E. Kandrup, Phys. Rev. E **60**, 1567 (1999). Figure 1 in that paper exhibits examples of ''sticky'' orbits in the potentials (3.1) and (3.2).
[17] Recall that, at least for a Gaussian distribution, the form of Γ is known to be irrelevant: any Γ that yields the correct autocorrelation time will yield the same estimated $\chi_{\rm est}$.
[18] Correlations between curvature and the rate of convergence for regular orbits are implicit in, e.g., Figs. 3–5 of Ref. [7].
[19] Equation (23) in M. Cerruti-Sola and M. Pettini, Phys. Rev. E **53**, 179 (1996).
[20] Unfortunately, an analytic solution using the approach discussed in Sec. IV seems impossible. For a single oscillator equation, one is led to three coupled moment equations and, hence, a cubic equation for χ. For two coupled oscillators, one has eight coupled equations and, hence, an eighth-order equation for χ.
[21] H. E. Kandrup, Astrophys. J. **500**, 120 (1998).
[22] C. L. Bohn, in *The Physics of High Brightness Beams*, edited by J. Rosenzweig and L. Serafini (World Scientific, Singapore, 2000), pp. 358–368.
[23] M. Cerruti-Sola and M. Pettini, Phys. Rev. E **53**, 179 (1996).
[24] T. deZeeuw, Mon. Not. R. Astron. Soc. **216**, 273 (1985).
[25] C. Siopis and H. E. Kandrup, Mon. Not. R. Astron. Soc. **319**, 43 (2000).
[26] H. E. Kandrup and I. V. Sideris, Phys. Rev. E (to be published). Discreteness effects in a chaotic potential, modeled as friction and noise, typically trigger an exponential divergence.
[27] M. Di Bari, D. Boccaletti, P. Cipriani, and G. Puccacio, Phys. Rev. E **55**, 6448 (1997).
[28] P. Cipriani and M. Di Bari, Phys. Rev. Lett. **81**, 5532 (1998).
[29] G. Gallavotti, J. Math. Phys. **41**, 4061 (2000).